Full article
doi.org/10.1002/elsa.202100007

Chemistry Europe
European Chemical Societies Publishing

Received: 10 January 2021
Revised: 22 March 2021
Accepted: 7 April 2021

Transport properties of imidazolium based ionic liquid electrolytes from molecular dynamics simulations

Moon Young Yang[1] | **Boris V. Merinov**[1] | **Sergey V. Zybin**[1] | **William A. Goddard III**[1] | **Eun Kyung Mok**[2] | **Hoe Jin Hah**[2] | **Hyea Eun Han**[2] | **Young Cheol Choi**[2] | **Seung Ha Kim**[2]

[1] Division of Chemistry and Chemical Engineering, Materials and Process Simulation Center, MC 139-74, California Institute of Technology, Pasadena, California, USA

[2] Battery R & D, LG Chem, Yuseong-Gu, Daejeon, Republic of Korea

Correspondence
Boris V. Merinov, Materials and Process Simulation Center, MC 139-74, California Institute of Technology, Pasadena, California 91125, USA.
Email: merinov@caltech.edu
William A. Goddard III, Materials and Process Simulation Center, MC 139-74, California Institute of Technology, Pasadena, California 91125, USA.
Email: wag@caltech.edu

Funding information
LG Chem, Grant/Award Number: CR18040404; InnoHK; National Science Foundation, Grant/Award Number: ACI-1548562

Abstract

Ionic liquids (ILs) are promising electrolytes for high-performance Li-ion batteries (LIBs), which can significantly improve the safety and energy storage capacity. Although extensive experimental and computational studies have reported, further exploration is needed to understand the properties of IL systems, their microscopic structures and dynamics, and the behavior of Li ions in ILs. We report here results of molecular dynamics simulations as a function of electric field for Li diffusion in two IL systems, [EMIM][TFSI] and [BMIM][TFSI] doped with various concentrations of LiTFSI. We find that the migration of each individual Li ion depends largely on its micro-environment, leading to differences by factors of up to 100 in the diffusivity. The structural and dynamical properties indicate that Li diffusion is affected significantly by the coordination and interaction with the oxygen species in the TFSI anions. Moreover, the IL cations also contribute to the Li diffusion mechanism by attenuating the Li–TFSI interaction.

KEYWORDS
battery, ion diffusion, ionic liquids, mobility

1 | INTRODUCTION

Rechargeable lithium-ion batteries (LIBs) have become one of the most important and widely-used electrical energy storage devices since their successful commercialization in the early 1990s.[1] Despite their excellent properties, there is a growing demand for a new generation of electrochemical storage systems with superior properties suitable for a number of applications including transportation. However, many challenges remain that must be overcome to develop a new generation of high-performance LIBs. One of the major obstacles is the safety issue caused by employing volatile/flammable lithium-salts/organic polar solvents as electrolytes,[2,3] which suffer from possible dendrite formation and leakage leading to explosion and fire.

Promising alternatives for conventional electrolytes are ionic liquids (ILs), generally defined as molten salts with a melting point below 100°C. They possess a number of excellent properties, such as high thermal

Full article
doi.org/10.1002/elsa.202100007
Chemistry Europe
European Chemical Societies Publishing

stability, non-volatility/flammability, high ionic conductivity, and a wide electrochemical stability range.[4,5] Bis(trifluoromethanesulfonyl)imide (TFSI) are the most widely used and well-studied IL anions.[6] The flexible S−N−S bonds in TFSI lowers both the melting point and viscosity while the electron-withdrawing CF_3SO_2 groups provide a large electrochemical stability window.[7,8] ILs combining of TFSI with imidazolium-based cations, such as 1-butyl-3-methylimidazolium (BMIM) or 1-ethyl-3-methylimidazolium chloride (EMIM), have received increasing attention due to their attractive properties such as relatively low viscosity and high conductivity.[8]

Since performance of electrochemical cells depends significantly on electrolyte, it is crucial to fully understand the physico-chemical processes in ILs under electrochemical conditions. Extensive experimental and computational studies have been conducted to elucidate the structural and ion transport characteristics of ILs,[9–13] because they are directly related to macroscopic properties such as viscosity, electrical conductivity, and chemical stability. It has been reported that ion self-diffusion coefficients in typical [BMIM][TFSI] or [EMIM][TFSI] IL are of the order of 10^{-11} m^2/s.[14,15] This diffusion is affected by the addition of Li salts, such as LiTFSI, $LiNO_3$, $LiPF_6$, and $LiBF_4$, with a gradually decrease observed as the Li salt concentration increases.[16] This occurs because the small size of the Li ion compared to that of the IL cation induces stronger interaction with anions. However, the IL ion diffusivity increases again at very high Li concentrations.[10]

Due to the complexity of ILs compared to common solvents, experimental approaches produce limited information on their structures and diffusion mechanisms, in particular at the atomistic level. In contrast, computational simulations are a powerful tool to investigate the properties of such complex systems to generate important information for developing new efficient electrolytes.[10,11,17–24] Here, molecular dynamics (MD) provides a most powerful means to investigate structural and dynamical properties of ILs, including dependence of ion behavior on additive salt concentration and external electric field.[10,19]

In this paper, we report the results of MD studies of two IL systems: [BMIM][TFSI] and [EMIM][TFSI] with various LiTFSI concentrations. In particular, we provide a detailed description of the structures and ion transport properties under ambient conditions and external electric field.

2 | COMPUTATIONAL METHODS

For our MD studies we selected two IL systems, [BMIM][TFSI] and [EMIM][TFSI] containing 192 ion pairs, with Li ion concentrations from 0 to 20% (rounded down to the nearest integer: 5%Li = 10 Li, 10%Li = 20 Li, 15%Li = 30 Li, and 20%Li = 40 Li) of the total number of the cations (192). All simulations were carried out using the OPLS2005 force field[25] with the LAMMPS software.[26]

The initial models for [BMIM][TFSI] and [EMIM][TFSI] were prepared based on their crystal structures,[27,28] which were minimized and equilibrated by the following procedure. The equilibration step consisted of

a. NVT (constant number of molecules, volume, and temperature) MD simulation at 10 K for 10 ps to generate initial velocities,
b. heating from 10 K to 300 K for 100 ps. For activation energy calculations, we also heated to 375 K and 450 K over 100 ps,
c. NPT (constant number of molecules, pressure, and temperature) MD simulation at the target temperature for 1 ns to optimize cell parameters and density of the system, and
d. NVT MD simulation for 1 ns with the density obtained in step c to equilibrate the system.

After equilibration, 5 ns of NVT MD was performed on the IL model structures. For nonpolarizable force fields, simulations of ILs with the ±1e ion charge often fail to reproduce the transport properties because of neglecting electronic effects such as polarization and charge transfer.[29] Charge scaling is an efficient way to approximately include those effects without further computational cost.[30] In this study, we applied a total charge of +0.7e to each BMIM or EMIM cation, and −0.7e for the TFSI anion. Li charge was also scaled to +0.7e for the charge neutrality. The scaled point charges on each atom were assigned based on the QM-based electrostatic potential (ESP) calculation (Figure S1), where [Li][TFSI] and [TFSI][BMIM/EMIM] pairs were used, and all geometries were fully optimized at the B3LYP/6-31G(d,p) level using the Gaussian 09 program.[31]

The transport properties of ions in MD simulations are usually measured by the self-diffusion coefficient (D) from the mean square displacement (MSD):

$$MSD\ (t) = \lim_{t\to\infty} \langle |r_i(t) - r_i(t_0)| \rangle^2 = 6Dt, \qquad (1)$$

where $r_i(t)$ is the position of ion i (center of mass for cations/anions) at time t and t_0 is the reference time. We identified the Fickian regime for each MSD curve (Figure S2) to calculate the ion diffusion coefficients. The largest domain, τ, where the log−log slope is nearly unity, is selected as the fitting region.

We also calculated the effect of electric fields by applying DC fields to the IL bulk structures from 0 to 0.1 V/Å along the x direction. Electric fields were applied as a

Full article
doi.org/10.1002/elsa.202100007
Chemistry Europe
European Chemical Societies Publishing

TABLE 1 Density (kg/m^3) of ILs as a function of the Li concentration

		Li concentration (%)				
	Exp. (pure IL)[14,32]	0	5	10	15	20
[BMIM][TFSI]	1438	1470	1484	1493	1505	1522
[EMIM][TFSI]	1517	1538	1555	1571	1582	1592

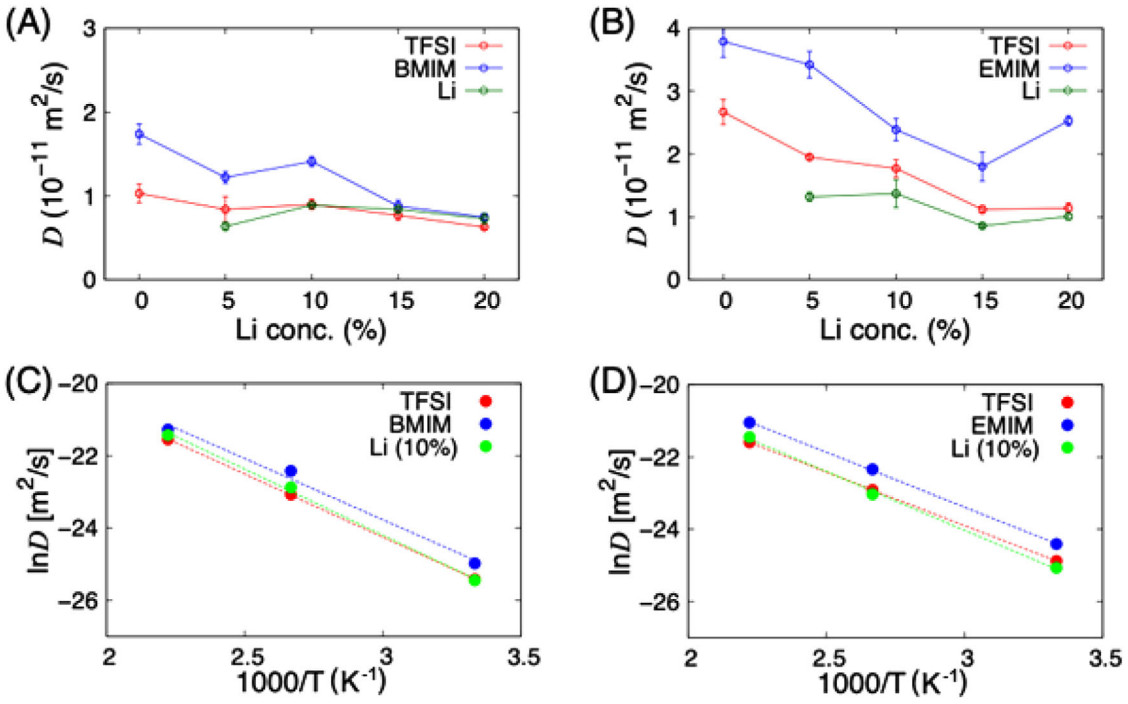

FIGURE 1 Ion diffusivities of the (A) [BMIM][TFSI] and (B) [EMIM][TFSI] ILs with various Li concentrations and Arrhenius plots of the ion diffusivities in (C) [BMIM][TFSI] and (D) [EMIM][TFSI] as a function of 1000/T. Activation energies for ion diffusions were estimated from the slopes of the linear fits

static force to each particle of F = qE, where q is the charge on the particle and E is the electric field strength (see more detailed information on this procedure in the LAMMPS manual[26]). We used periodic boundary conditions, with the local E equal to the applied electric field strength.

3 | RESULTS AND DISCUSSION

3.1 | Ion diffusion in ionic liquids with various Li concentrations

The densities (ρ) of the selected IL systems, [BMIM][TFSI] and [EMIM][TFSI], were calculated as a function of the Li concentration (Table 1). They are higher than the experimental ones, by 2% and 1%, respectively,[14,32] and increase gradually with increasing the Li concentration. This is in good agreement with reported experimental and theoretical studies[10,33] and can be interpreted in terms of stronger interactions between Li^+ and $[TFSI]^-$. Also, the shorter carbon chain of EMIM led to a density 4% higher than [BMIM][TFSI].

To investigate the transport property of each ion species, self-diffusion coefficients (D) were calculated from the MSD plots (Figure S2). Figures 1A and 1B show the predicted diffusion coefficients for various Li concentrations at 300 K. We also calculated the mobilities (μ) as

$$\mu = qD/k_BT,$$

where q – charge, k_B – Boltzmann's constant, and T – temperature, and listed the corresponding values in Table S1.

For the pure IL systems, the diffusion coefficients of the cation and anion are 1.74 and 1.03 × 10^{-11} m^2/s for [BMIM][TFSI], and 3.79 and 2.67 × 10^{-11} m^2/s for [EMIM][TFSI], respectively, which are in good agreement with experimental results, ranging from 2.4 to 4.8 × 10^{-11} m^2/s for cations and from 2.0 to 2.9 × 10^{-11} m^2/s for anions.[15,16,34] The diffusion coefficients of the IL cation

Full article
doi.org/10.1002/elsa.202100007
Chemistry Europe
European Chemical Societies Publishing

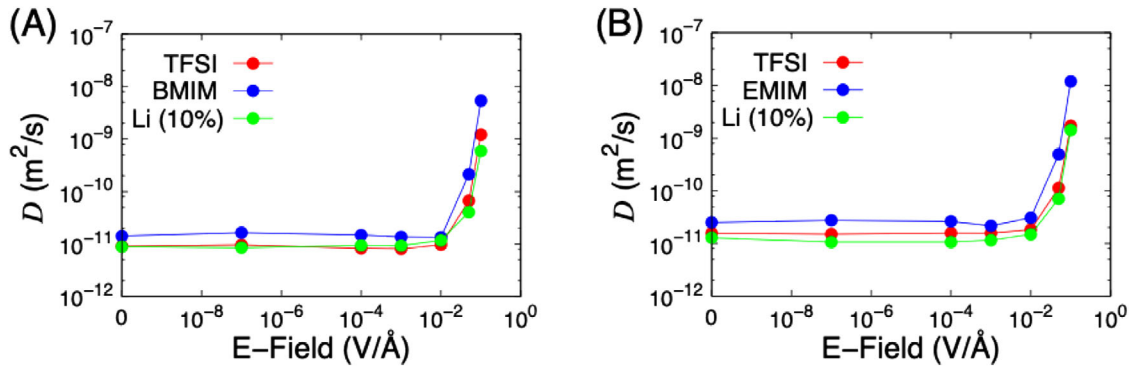

FIGURE 2 The diffusion coefficients for (A) [BMIM][TFSI] and (B) [EMIM][TFSI] systems at the 10%Li concentration under different strengths of electric field

and anion gradually decrease as the Li salt concentration increases. This is due to the increased viscosity of the ILs at higher Li-salt concentration.[10,35] Duluard *et al.* have reported the same trend using nuclear magnetic resonance (NMR) spectroscopy for [BMIM][TFSI], leading to diffusion constants from 1.0×10^{-11} m^2/s (pure IL) to 2.4×10^{-11} m^2/s (23%Li) for BMIM and from 0.6×10^{-11} m^2/s (pure IL) to 2.1×10^{-11} m^2/s (23%Li) for TFSI, respectively.[16]

For both systems, we find that Li diffusion increases slightly from 0 to 10%Li, the highest diffusion coefficient value, and then decreases with concentration at higher loading (Figures 1A and 1B). This trend is consistent with reported experimental results, where a distinct Li-diffusion peak was observed at 10 wt% for [EMIM][FSI][10] and a much less pronounced Li-diffusion peak could be distinguished at 5 wt% for [BMIM][TFSI].[16] Note that the trend changes at very high Li content, where the Li diffusivity increases again at Li concentrations over 30 wt%.[10] The relative self-diffusion coefficients are $D_{cation} > D_{anion} > D_{Li}$, which is consistent with reported experimental and theoretical data.[10,15,16] The small Li ions interact strongly with anions, resulting in slower diffusivity.

We estimated the activation energies from the Arrhenius plots at three temperatures (300, 375, and 450 K) for each IL system doped with 10%Li (Figures 1C and 1D, Table S2). The calculated activation energy for Li ion diffusion is 0.31 eV for [BMIM][TFSI] and 0.28 eV for [EMIM][TFSI], which are 0.1-0.2 eV higher than for the IL cation and anion diffusions. These values are in good agreement with 0.27 and 0.26 eV obtained by D'Agostino *et al.*[36] for [EMIM][TFSI], and Jayakody *et al.*[37] for [BMIM][TFSI] using 0.5 M LiTFSI, with 0.35, 0.34, and 0.31 eV for Li, BMIM, and TFSI, respectively. Similar activation energies have been reported for other IL systems.[12]

3.2 | Ion diffusion in ionic liquids under electric field

In real batteries, an electrolyte is sandwiched between two electrodes, producing a voltage across a cell. Thus, it is important to understand how IL ions behave under external electric fields (E-field). To investigate the effect of the E-field on transport properties of ions, we performed MD simulations under various E-field strengths, from 0 to 0.1 V/Å, along the *x* direction. Note that the E-field in real batteries are generally <0.001 V/Å. However, modeling these materials under strong E-fields is of interest to provide a deeper insight into the ion behavior under extreme conditions.

Figure 2 shows the predicted diffusion coefficients for each ion species as a function of E-field strength with the corresponding calculated mobilities listed in Table S3. We find that for E-fields less than 10^{-2} V/Å, ion diffusion in both IL systems is barely affected by the magnitude of E, whereas ion diffusion increases drastically for E-fields stronger than 10^{-2} V/Å. An analogous trend was observed for all Li concentrations studied here (Figure S3). Similar results have been reported for theoretical calculations on other systems.[19,38]

Note that using a standard thermostat may cause interference along the E-field direction. However, as it was shown by Petravic,[39] this effect becomes apparent only at extremely high E-fields (>0.5 V/Å) and imposing a thermostat only on motion perpendicular to the E-field direction provides controlling the temperature of a system without any interference with the development of current. To be confident that the interference is negligible in our simulations, we performed additional computations on the [BMIM][TFSI] system with 10%Li under the 0.01 and 0.1 V/Å E-field (the strongest in our simulations), in which the thermostat was applied only along

Full article
doi.org/10.1002/elsa.202100007
Chemistry Europe
European Chemical Societies Publishing

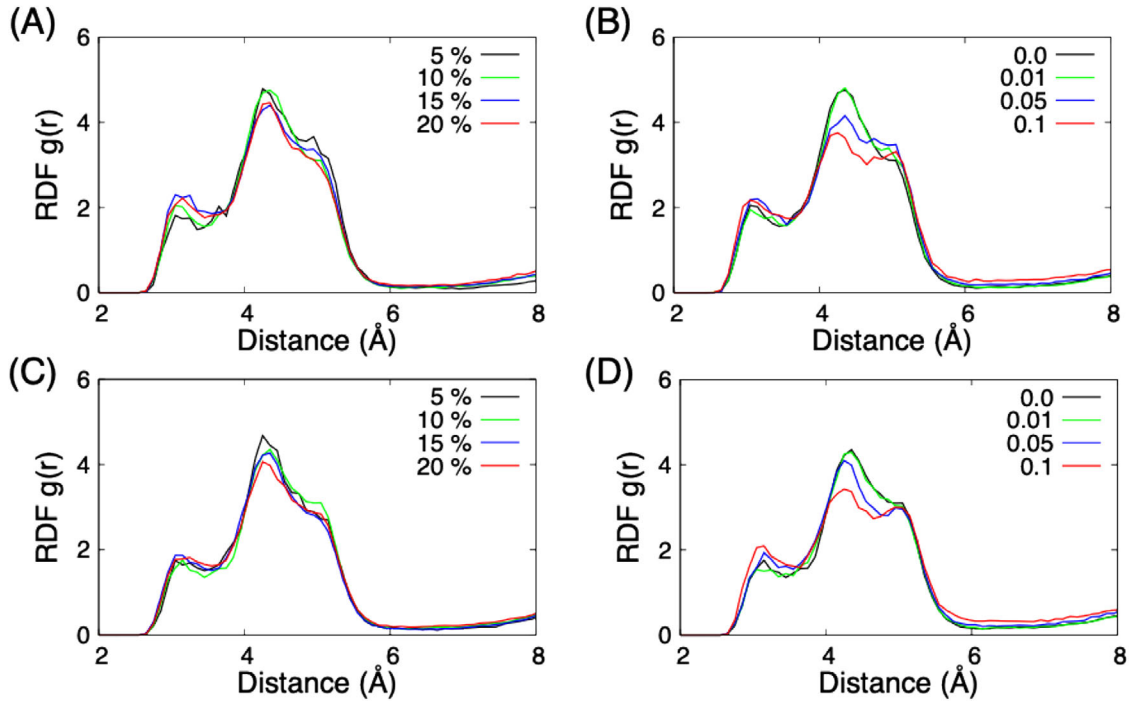

FIGURE 3 Radial distribution function (RDF) of the Li-N_{TFSI} pair for the (A, B) BMIM-TFSI and (C, D) EMIM-TFSI systems at various Li concentrations (A, C) without E-field and (B, D) under various E-field strengths (V/Å) for the 10%Li concentration

the *y* and *z* directions perpendicular to the E-field along the *x* direction. We obtained the essentially same diffusion coefficients as before using the standard thermostat (Figure S4).

Our result demonstrates that the effect of E-field on ion diffusion can be neglected for real energy storage devices, although the complexity of heterogenous environments, in particular at interfaces, should be analyzed carefully.

3.3 | Structural analysis of ionic liquids

To explore how interactions of Li with IL anions and cations are modified from adding Li salt or applying E-field, we calculated the radial distribution functions (RDFs) (Figures S5 and S6). Among the calculated RDFs, the Li-N_{TFSI} (nitrogen atom in TFSI) RDF shows the most significant changes (Figure 3). The RDF exhibits three major peaks at around 3.1, 4.3, and 5.1 Å, corresponding to different configurations between Li and TFSI molecules. In particular, we find different interactions with the oxygen species in TFSI (Figure S7). Typically, the middle peak at 4.3 Å indicates that the Li ion interacts with two oxygens of a TFSI molecule (bidentate coordination), whereas the other two peaks indicate that the Li ion interacts with one oxygen of a TFSI molecule (monodentate coordination). The intensity of the middle peak gradually decreases with increasing Li concentration or E-field strength, whereas the intensities of the other peaks at 3.1 Å and 5.1 Å increase slightly. This change implies that the number of bidentate configurations decreases as the Li concentration or E-field strength increases. In addition, this change in the Li–TFSI interactions can be related to a flexible anion conformation, that is, *cis* and *trans* isomers. The C-S-S-C dihedral angle distribution in TFSI shows that the ratio of *cis*-isomer increases at higher Li concentrations and for stronger E-fields (Figure S7), which is consistent with our earlier conclusion that the anion conformation can be changed by both Li concentration[10] and E-field strength.[19] We observed different peak positions in C-S-S-C dihedral angles in the [BMIM][TFSI] and [EMIM][TFSI] systems (Figure S8), indicating that the length of the IL cation side chain affects the TFSI conformation.

3.4 | Diffusion of individual Li in ionic liquids

To understand the Li transport in ILs in more detail, the self-diffusion of each individual Li ion was analyzed. We showed that the transport properties obtained from our 5 ns MD simulations in terms of densities, activation energies, and self-diffusion coefficients are in good agreement with experimental data.[14] But we find that diffusion of individual Li ions varies by up to two orders of magnitude

Full article
doi.org/10.1002/elsa.202100007
Chemistry Europe
European Chemical Societies Publishing

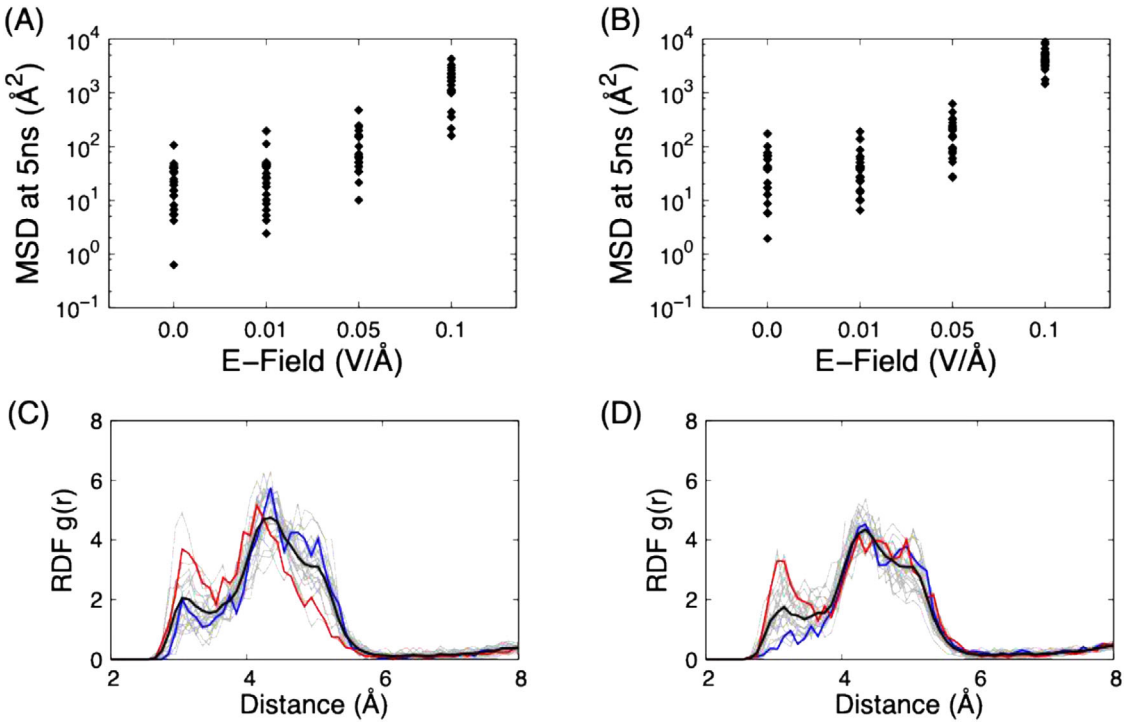

FIGURE 4 MSD values of each Li ion at 5 ns for (A) [BMIM][TFSI] and (B) [EMIM][TFSI] systems with 10%Li. Li-N_{TFSI} pair RDFs of each Li (thin gray lines) for (C) [BMIM][TFSI] and (D) [EMIM][TFSI] with 10%Li. The RDF for the fastest Li is shown by the red line, while the slowest Li is shown by the blue line. The average over all Li is shown by the black line

(Figures 4A, 4B and S9). Without the E-field, the maximum Li MSD is 105.9 Å^2 while the minimum is 0.6 Å^2 for [BMIM][TFSI], with 173.2 Å^2 and 1.9 Å^2 for [EMIM][TFSI], respectively. As expected, the overall MSD of each Li ion increases gradually as the E-field increases from 0 to 0.05 V/Å but then for E-field strengths over 0.05 V/Å, it increases abruptly. Note that the corresponding MSD values are distributed over a wide range of values (Figures 4A and 4B). Although the width of this range decreases with increasing the E-field strength, there is a large difference between the MSD maximum and minimum, 4273.2 Å^2 vs 160.0 Å^2 for [BMIM][TFSI], and 8821.9 Å^2 vs 1462.7 Å^2 for [EMIM][TFSI]. This means that individual Li ions diffuse very differently, depending on the micro-environment of each individual Li. The fast Li ions are characterized by a very intense Li-N_{TFSI} RDF peak at 3.1 Å or 5.1 Å (Figures 4C, 4D and S10). This indicates that the fast Li ions tend to interact with only one oxygen of a TFSI molecule, which is apparently more favorable for fast ion diffusion than the more rigid interaction with two oxygens of a TFSI molecule, which corresponds to the peak at 4.3 Å.

The 5 ns MSDs and trajectories of the most and least diffusive Li ions with the surrounding IL molecules are shown in Figure 5. The least diffusive Li ion occupies a position in a closed rigid cage formed by three TFSI molecules with bidentate coordination. In contrast, the most diffusive Li ion is in an open flexible cage of TFSI molecules, allowing it to move out of the cage at certain favorable conditions. This makes this cage more open due to interactions with TFSI anions and neighboring IL cations. During the 5 ns MD simulation, the least diffusive Li ion dangled within the closed cage of the TFSI molecules, moving slightly together with the cage (vehicular diffusion) (Figure 5B), whereas the most diffusive Li ion undergoes two big jumps, corresponding to hopping from one cage to another. Figure 5C shows the trajectory of the most diffusive Li ion, which stretches over three different cages. It can be partitioned into three intervals: 0–1.8 ns, 1.8-2.9 ns, and 2.9-5 ns. Our results indicate that individual Li diffusion depends strongly on its micro-environment with two types of the diffusion mechanisms for Li ions in ILs: vehicular (slow diffusion) and hopping (fast diffusion). These mechanisms were first described in the study of solutes in ILs,[40,41] and then similar results have been reported in recent experimental and computational works.[20,42]

We also observed very different diffusion behaviors of individual Li ions under E-field (Figure 6). For the zero and 0.01 V/Å E-field cases, the least diffusive Li ion barely moved during the 5 ns MD simulations, while the most diffusive Li ions showed significant migration through hopping several times. It should be noted that the E-field was applied along the *x*-axis, whereas the most diffusive Li ion migrated roughly along the *z*-axis. This demonstrates that

Full article
doi.org/10.1002/elsa.202100007
Chemistry Europe
European Chemical Societies Publishing

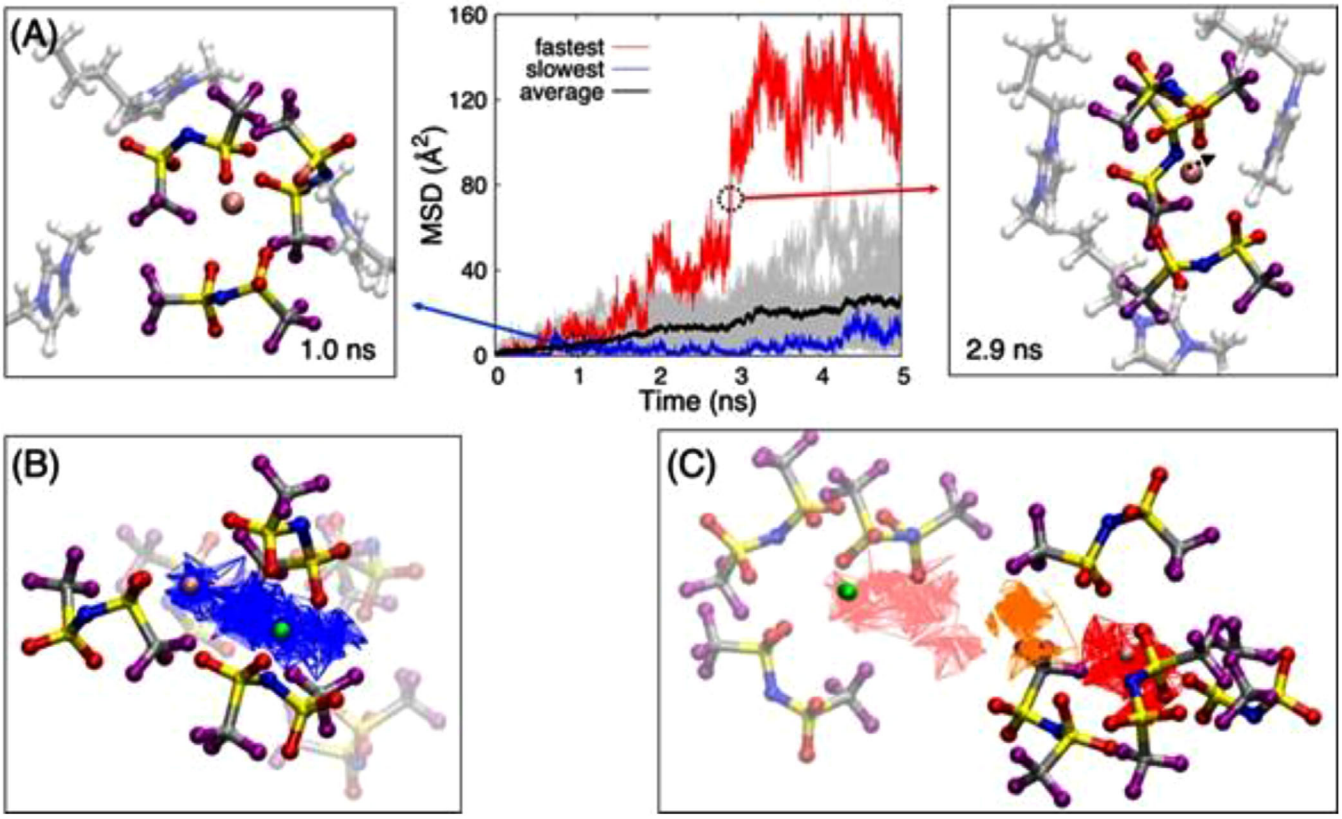

FIGURE 5 Diffusion of individual Li ions in [BMIM][TFSI] with 10%Li. (A) MSD plots of individual Li (middle) with the local environments around the fastest (right) and slowest (left) Li at 2.9 and 1.0 ns, respectively. (B and C) The whole 5 ns trajectories for the diffusion of the slowest and fastest Li, respectively, where the transparent TFSI molecules indicate the initial TFSI configuration, while the solid ones indicate the final configuration around Li. The green and pink spheres show the initial and final positions of the slowest and fastest Li ions. The fastest Li spreads over three different cages for 0–1.8 ns (pink), 1.8-2.9 ns (orange), and 2.9-5 ns (red)

an E-field < 0.01 V/Å is too weak to affect the structural and dynamic properties of the systems. Under stronger E-fields, 0.05 V/Å and 0.1 V/Å, the fast transport of the most diffusive Li ion occurs by frequent hopping along the E-field direction. Interestingly, even under these high E-field strengths, the least diffusive Li ion moves slowly, indicating that interactions between the Li and IL ions governed by the micro-environments significantly affect the Li diffusion.

4 | CONCLUSION

We performed MD simulations to investigate Li diffusion in the [BMIM][TFSI] and [EMIM][TFSI] ILs with various Li concentrations and under various E-fields. The estimated diffusion coefficients of the ion species in both systems are in good agreement with available experimental results. We find that the diffusion of each individual Li ion depends strongly on its micro-environment, with 100-fold differences.

Our computational studies reveal that Li diffusion is affected significantly by interactions between the IL ions, in particular by the coordination and interaction of Li with the oxygen species of the IL anions. Moreover, the IL cations contribute to Li transport by interacting with the TFSI anions to create favorable conditions for Li hopping. The fast Li-ion diffusion occurs *via* the hopping mechanism, with Li-ions jumping from one cage to another, while the Li-ion diffusion *via* the vehicular mechanism is slow. The ion diffusion is affected only slightly under E-fields less than 0.05 V/Å.

The complexity of heterogenous environments and interfaces should be considered carefully to fully understand the effect of the E-field on the structure and properties of an electrochemical cell.

These insights into the Li diffusion process at the atomistic level provide essential information for developing advanced electrolyte materials for a new generation of high performance LIBs.

ACKNOWLEDGMENTS

This work was initiated by a research grant from LG Chem. It was completed with support provided by InnoHK. We used the Extreme Science and Engineering Discovery Environment (XSEDE) system, which is

Full article
doi.org/10.1002/elsa.202100007
Chemistry Europe
European Chemical Societies Publishing

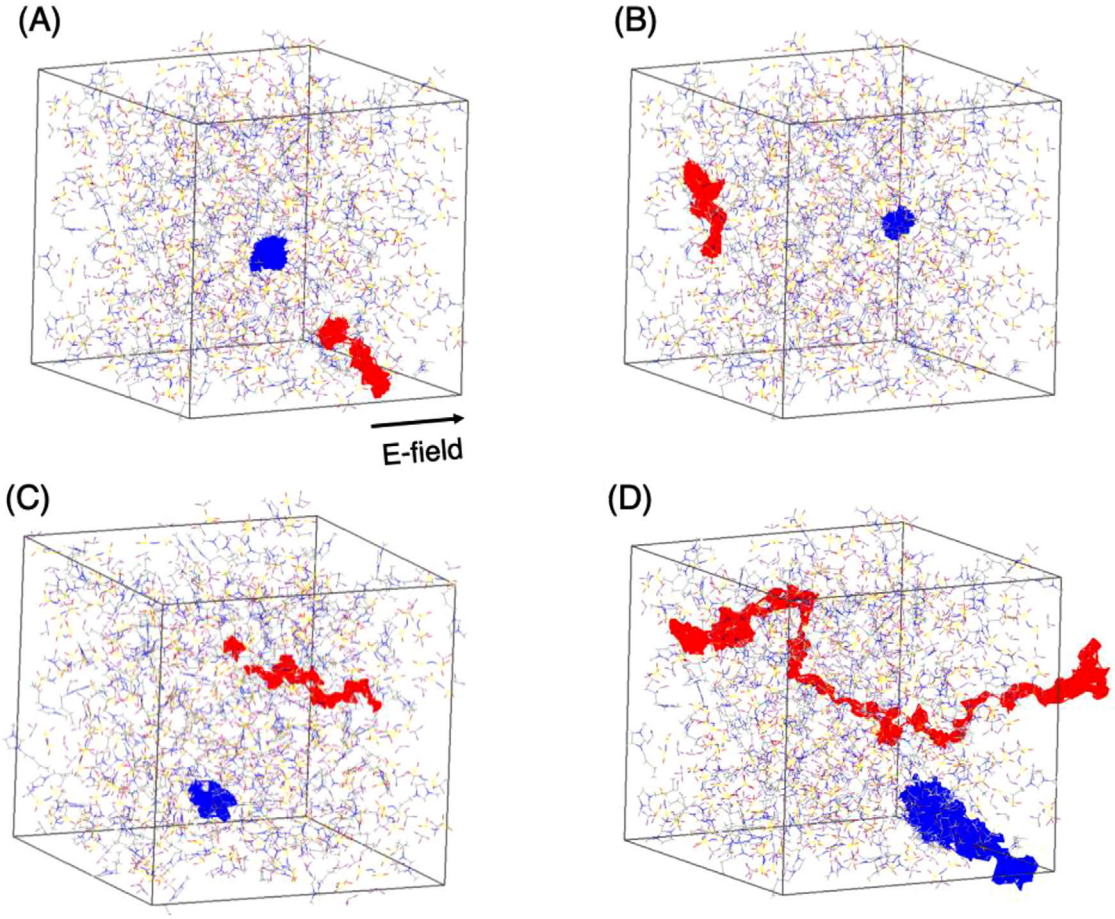

FIGURE 6 Trajectories of the most diffusive (red) and least diffusive (blue) Li ion in the [TFSI][BMIM] system with 10%Li under E-field of (A) 0 V/Å, (B) 0.01 V/Å, (C) 0.05 V/Å, and (D) 0.1 V/Å. The E-field was applied along the *x*-axis

supported by National Science Foundation, grant ACI-1548562.

DATA AVAILABILITY STATEMENT

Data available on request from the authors.

ORCID

Boris V. Merinov https://orcid.org/0000-0002-2783-4262

REFERENCES

1. J. B. Goodenough, Y. Kim, *J. Power Sources* **2011**, *196*, 6688.
2. V. Etacheri, R. Marom, R. Elazari, G. Salitra, D. Aurbach, *Energy Environ. Sci.* **2011**, *4*, 3243.
3. L. Lu, X. Han, L. Jianqiu, J. Hua, *J. Power Sources* **2012**, *226*, 272.
4. M. Galinski, A. Lewandowski, I. Stepniak, *Electrochim. Acta* **2006**, *51*, 5567.
5. A. Lewandowski, A. Swiderska-Mocek, *J. Power Sources* **2009**, *194*, 601.
6. M. V. Fedorov, A. A. Kornyshev, *Chem. Rev.* **2014**, *114*, 2978.
7. S. Zhang, N. Sun, X. He, X. Lu, X. Zhang, *J. Phys. Chem. Ref. Data* **2006**, *35*, 1475.
8. M. Armand, F. Endres, D. R. MacFarlane, H. Ohno, B. Scrosati, *Nat. Mater.* **2009**, *8*, 621.
9. G. A. Elia, U. Ulissi, S. Jeong, S. Passerini, J. Hassoun, *Energy Environ. Sci.* **2016**, *9*, 3210.
10. J. Tong, S. Wu, N. von Solms, X. Liang, F. Huo, Q. Zhou, H. He, S. Zhang, *Front. Chem.* **2020**, *7*, 945.
11. K. Oldiges, D. Diddens, M. Ebrahiminia, J. B. Hooper, I. Cekic-Laskovic, A. Heuer, D. Bedrov, M. Winter, G. Brunklaus, *Phys. Chem. Chem. Phys.* **2018**, *20*, 16579.
12. S. Indris, R. Heinzmann, M. Schulz, A. Hofmann, *J. Electrochem. Soc.* **2014**, *161*, A2036.
13. H. Yoon, P. C. Howlett, A. S. Best, M. Forsyth, D. R. MacFarlanea, *J. Electrochem. Soc.* **2013**, *160*, A1629.
14. H. Tokuda, K Hayamizu, K. Ishii, M A. B. H. Susan, M. Watanabe, *J. Phys. Chem. B* **2005**, *109*, 6103.
15. T. Umecky, Y. Saito, H. Matsumoto, *J. Phys. Chem. B* **2009**, *113*, 8466.
16. S. Duluard, J. Grondin, J.-L. Bruneel, I. Pianet, A. Grelard, G. Campet, M.-H. Delville, J.-C Lassegues, *J. Raman Spectrosc.* **2008**, *39*, 627.
17. B. V. Merinov, S. V. Zybin, S. Naserifar, S. Morozov, J. Oppenheim, W. A. Goddard III, J. Lee, J. H. Lee, H. E. Han, Y. C. Choi, S. H. Kim, *J. Phys. Chem. Lett.* **2019**, *10*, 4577.
18. B. V. Merinov, S. Naserifar, S. V. Zybin, S. Morozov, W. A. Goddard III, J. Lee, J. H. Lee, H. E. Han, Y. C. Choi, S. H. Kim, *J. Chem. Phys.* **2020**, *152*, 031101.

19. R. Clark, M. von Domaros, A. J. S. McIntosh, A. Luzar, B. Kirchner, T. Welton, *J. Chem. Phys.* **2019**, *151*, 164503.
20. G. Feng, M. Chen, S. Bi, Z. A. H. Goodwin, E. B. Postnikov, N. Brilliantov, M. Urbakh, A. A. Kornyshev, *Phys. Rev.* **2019**, *X9*, 021024.
21. N. Molinari, J. P. Mailoa, B. Kozinsky, *J. Phys. Chem. Lett.* **2019**, *10*, 2313.
22. D. Bedrov, J.-P. Piquemal, O. Borodin, A. D. MacKerell Jr., B. Roux, C. Schröder, *Chem. Rev.* **2019**, *119*, 7940.
23. Z. Li, O. Borodin, G. D. Smith, D. Bedrov, *J. Phys. Chem. B* **2015**, *119*, 3085.
24. J. G. McDaniel, C. Y. Son, A. Yethiraj, *J. Phys. Chem. B* **2018**, *122*, 4101.
25. J. L. Banks, H. S. Beard, Y. Cao, A. E. Cho, W. Damm, R. Farid, A. K. Felts, T. A. Halgren, D. T. Mainz, J. R. Maple, R. Murphy, D. M. Philipp, M. P. Repasky, L. Y. Zhang, B. J. Berne, R. A. Friesner, E. Gallicchio, R. M. Levy, *J. Comput. Chem.* **2005**, *26*, 1752.
26. S. Plimpton, *J. Comp. Phys.* **1995**, *117*, 1.
27. A. R. Choudhury, N. Winterton, A. Steiner, A. I. Cooper, K. A. Johnson, *Crys. Eng. Comm.* **2006**, *8*, 742.
28. A. V. Blokhin, Y. U. Paulechka, A. A. Strechan, G. J. Kabo, *J. Phys. Chem. B* **2008**, *112*, 4357.
29. M. Salanne, *Phys. Chem. Chem. Phys.* **2015**, *17*, 14270.
30. T. G. A. Youngs, C. Hardacre, *Chem. Phys. Chem.* **2008**, *9*, 1548.
31. M. J. Frisch, G. W. Trucks, H. B. Schlegel, G. E. Scuseria, M. A. Robb, J. R. Cheeseman, G. Scalmani, V. Barone, B. Mennucci, G. A. Petersson, H. Nakatsuji, M. Caricato, X. Li, H. P. Hratchian, A. F. Izmaylov, J. Bloino, G. Zheng, J. L. Sonnenberg, M. Hada, M. Ehara, K. Toyota, R. Fukuda, J. Hasegawa, M. Ishida, T. Nakajima, Y. Honda, O. Kitao, H. Nakai, T. Vreven, J. A. Montgomery Jr., J. E. Peralta, F. Ogliaro, M. Bearpark, J. J. Heyd, E. Brothers, K. N. Kudin, V. N. Staroverov, R. Kobayashi, J. Normand, K. Raghavachari, A. Rendell, J. C. Burant, S. S. Iyengar, J. Tomasi, M. Cossi, N. Rega, J. M. Millam, M. Klene, J. E. Knox, J. B. Cross, V. Bakken, C. Adamo, J. Jaramillo, R. Gomperts, R. E. Stratmann, O. Yazyev, A. J. Austin, R. Cammi, C. Pomelli, J. W. Ochterski, R. L. Martin, K. Morokuma, V. G. Zakrzewski, G. A. Voth, P. Salvador, J. J. Dannenberg, S. Dapprich, A. D. Daniels, O. Farkas, J. B. Foresman, J. V. Ortiz, J. Cioslowski, D. J. Fox, Gaussian 09, Revision A.1, Gaussian, Inc. Wallingford CT, **2009**.
32. K. Fujii, Y. Soejima, Y. Kyoshoin, S. Fukuda, R. Kanzaki, Y. Umebayashi, T. Yamaguchi, S. Ishiguro, T. Takamuku, *J. Phys. Chem. B* **2008**, *112*, 4329.
33. M. J. Monteiro, F. F. C. Bazito, L. J. A. Siqueira, M. C. C. Ribeiro, R. M. Torresi, *J. Phys. Chem. B* **2008**, *112*, 2102.
34. S. Tsuzuki, *ChemPhysChem* **2012**, *13*, 1664.
35. S. Seki, Y. Ohno, Y. Kobayashi, H. Miyashiro, A. Usami, Y. Mita, H. Tokuda, M. Watanabe, K. Hayamizu, S. Tsuzuki, M. Hattori, N. Terada, *J. Electrochem Soc.* **2007**, *154*, A173.
36. C. D'Agostino, M. D. Mantle, C. L. Mullan, C. Hardacre, L. F. Gladden, *ChemPhysChem* **2018**, *19*, 1081.
37. N. K. Jayakody, C. C. Fraenza, S. G. Greenbaum, D. Ashby, B. S. Dunn, *J. Phys. Chem. B* **2020**, *124*, 6843.
38. N. J. English, D. A. Mooney, S. O'Brien, *Mol. Phys.* **2011**, *109*, 625.
39. J. Petravic, *J. Chem. Phys.* **2003**, *118*, 7477.
40. J. C. Araque, J. J. Hettige, C. J. Margulis, *J. Phys. Chem. B* **2015**, *119*, 12727.
41. A. Kaintz, G. Baker, A. Benesi, M. Maroncelli, *J. Phys. Chem. B* **2013**, *117*, 11697.
42. K. Dokko, D. Watanabe, Y. Ugata, M. L. Thomas, S. Tsuzuki, W. Shinoda, K. Hashimoto, K. Ueno, Y. Umebayashi, M. Watanabe, *J. Phys. Chem. B* **2018**, *122*, 10736.

SUPPORTING INFORMATION

Additional supporting information may be found online in the Supporting Information section at the end of the article.

How to cite this article: M. Y. Yang, B. V. Merinov, S. V. Zybin, W. A. Goddard, E. K. Mok, H. J. Hah, H. E. Han, Y. C. Choi, S. H. Kim. Transport properties of imidazolium based ionic liquid electrolytes from molecular dynamics simulations. *Electrochem Sci Adv*. **2021**;e2100007. https://doi.org/10.1002/elsa.202100007